

Guest inclusion in cyclic imides containing flexible tethers

Devendra Singh · Jubaraj B. Baruah

Received: 13 August 2011 / Accepted: 5 June 2012 / Published online: 23 June 2012
© Springer Science+Business Media B.V. 2012

Abstract Guest inclusion properties of two cyclic imides which have carboxylic acids connected through flexible tether, namely, 4-(1,3-dioxo-1,3-dihydro-isoindol-2-ylmethyl)-cyclohexanecarboxylic acid (**1**) and 4-(1,3-dioxo-1*H*, 3*H*-benzo[*de*]isoquinolin-2-ylmethyl)-cyclohexanecarboxylic acid (**2**) are studied. The crystals of host **1** containing one molecule of **1**, the crystals of 4,4'-bipyridine (bpy) cocrystal of **1** containing one molecule of **1** and half molecule of bpy (**1a**), the crystals of 1,4-dioxane solvate of **1** containing two molecule of **1** and one and half molecule of 1,4-dioxane (**1b**) and the crystals of quinoline solvate of **1** containing one molecule of **1** and one molecule of quinoline (**1c**) in their crystallographic asymmetric units are investigated. Intermolecular hydrogen bonded two dimensional (2D) sheet structure of **1** and 3D channel network of **1b** are comprised of cyclic $R_2^2(8)$ hydrogen bond motifs; whereas cleavage of dimeric carboxylic acid $R_2^2(8)$ motifs occurs in the structures of **1a** and **1c** in which 3D host–guest networks are comprised of discrete O–H...N and cyclic $R_2^2(7)$ interactions, respectively. Various types of weak interactions between the two symmetry nonequivalent host molecule are found to be responsible for the formation of channels ($14 \times 11 \text{ \AA}$) filled by guest 1,4-dioxane molecules in the crystal lattice of **1b**. Two different solvates of **2** containing one molecule of **2** with a water molecule (**2a**) and one molecule of **2** with a quinoline molecule (**2b**) in their crystallographic asymmetric units,

respectively, are also crystallized in different space groups. The quinoline molecules are held with host molecules by discrete O–H...N and C–H...O interactions and reside inside the voids formed by 3D repeated hexameric assemblies of host molecules in the crystal lattice of **2b**.

Keywords Cyclic imides · Flexible tethered carboxylic acids · Cocrystals · Channel formation · Guest inclusion · Structural study

Introduction

Rational design of molecular assemblies using organic functional solids to generate a variety of supramolecular architectures has gained impressive research interest in the field of crystal engineering and supramolecular chemistry [1–10]. Host–guest crystalline materials are of special interest in solid state due to their different physical properties from corresponding hosts [11–16] which makes them useful as pharmaceutical applications [17–20]. In particular, the development of host–guest microporous materials with channels and cavities are important because they have possible applications in the areas of heterogeneous catalysis, size selective separation, gas absorption and biomedicines [21–28]. In the field of supramolecular chemistry, cyclic imide derivatives are proved as versatile scaffolds to design the crystals of specific molecular arrangements [29–39]. Cyclic imides attached to aromatic rings possess dipolar nature and this effect provide extra stability to the packing arrangement [40, 41]. The basic difference between phthalimide and naphthalimide as hosts from other related cyclic imides that are without an aromatic part is that the former two are bipolar; can lead to interesting layered structures. Attachment of a carboxylic acid through

Electronic supplementary material The online version of this article (doi:10.1007/s10847-012-0196-7) contains supplementary material, which is available to authorized users.

D. Singh · J. B. Baruah (✉)
Department of Chemistry, Indian Institute of Technology
Guwahati, Guwahati 781 039, Assam, India
e-mail: juba@iitg.ernet.in

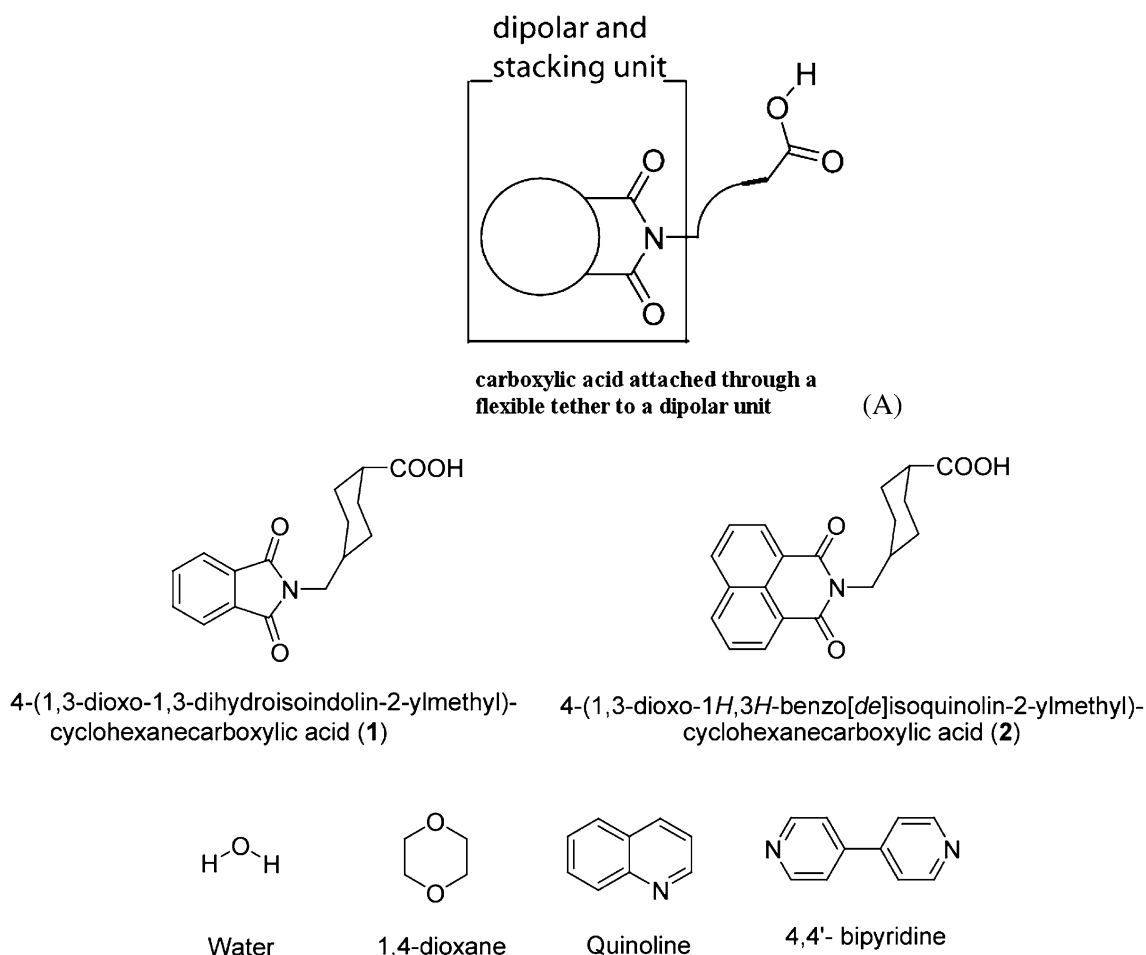


Chart 1 Structures of cyclic imide tethered carboxylic acids **1** and **2** and guest molecules

a hydrophobic part with flexibility to such part would enhance possibilities to adopt different structures through conformations guided by the competition between various weak interactions. From this point of view, imides attached to aromatic rings such as phthalimides, naphthalimides draw special interest as they serve as model for understanding hierarchical weak interactions [42]. Extensive study on supramolecular chemistry of derivatives of such compounds is available [43–54], but the effect on use of hydrophobic unit such as cyclohexyl group with conformational flexibility coupled with imide group would be of great interest [55]. Such study may also help to design new hosts with specific properties as obtained from calix-arene functionalized phthalimide derivatives [56–58].

With this objective, we have studied the host–guest chemistry of phthalimide and naphthalimide derivatives **1** and **2** which have intervening cyclohexyl moiety which can have flexible geometry while anchoring imide and carboxylic acid functionality at 1,4 transpositions with guest molecules like water, 1,4-dioxane, quinoline, 4,4'-bipyridine (Chart 1). The guest molecules chosen such that they have the prerequisites to interact with carboxylic acids

through hydrogen bond, and also to interact with the cyclic imide part by interactions such as hydrogen bonding (strong or weak) or through an aromatic part by weak C–H... π or π – π interactions. Carboxylic acid groups can form cyclic or discrete hydrogen bond motifs in several ways when they interact to each other or with guest molecules such as pyridine, quinoline and 1,4-dioxane [59–61]. Some of the host–guest cyclic or discrete hydrogen bond motifs expected to observe from such study, are shown in Chart 2. There are examples in literature in which macrocycles are functionalized across two ends and extended structures are demonstrated, in such cases the advantages of various hydrogen bond parameters based on distances and angles are used to establish the formation of such structure, here also we adopt a similar methodology by determining the structures of various host–guest systems [62–64].

Results and discussion

Two cyclic imide tethered with a cyclohexyl intervening groups containing carboxylic acids, **1** and **2**, are obtained

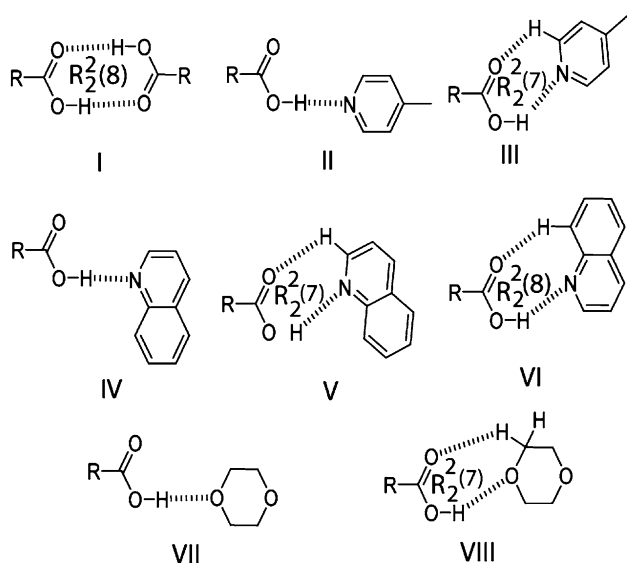


Chart 2 Some hydrogen bond motifs between carboxylic acid groups and guest molecules

by direct [1 + 1] cyclo-condensation reactions of trans-4-(aminomethyl)cyclohexanecarboxylic acid with corresponding anhydrides. Crystallization of **1** under different conditions led to the formation of four different types of crystals of **1**. The guest free crystals of **1** are obtained by crystallizing **1** from dry ethanol solvent, crystals of cocrystal **1a** are obtained in a mixture of dry ethanol and dry chloroform solvents containing **1** and bpy in 2:1 ratio, and the crystals of two different solvates, **1c** and **1d**, are obtained from 1,4-dioxane and quinoline solution of **1**, respectively (Scheme 1). All the parent compounds are characterized by recording their NMR, IR, mass spectra. The compositions of each solvates are ascertained from their proton NMR integrations. Each of the compounds has their characteristic IR signature of the parent compounds and of the guest molecules.

The compound **1** crystallized in monoclinic $P2_1/c$ space group, possesses one molecule of **1** in its crystallographic asymmetric unit (Fig. 1). In the crystal lattice of **1**, $-\text{COOH}$ groups interact to each other by the combination of two donor-acceptor $\text{O}-\text{H}\cdots\text{O}$ ($\text{O2}-\text{H2}\cdots\text{O1}$; $d_{\text{D}\cdots\text{A}}$ 2.66 Å, $\angle\text{D}-\text{H}\cdots\text{A}$ 177.54°) interactions creating 1D zigzag chains with lengths of 21.75 Å (measured from the center of the aromatic imide ring to the center of the aromatic imide ring). The acceptor oxygen atom of $-\text{COOH}$ group also participates in bifurcated hydrogen bonding and further interacts with hydrogen atom of aromatic imide ring via $\text{C}-\text{H}\cdots\text{O}$ ($\text{C11}-\text{H11}\cdots\text{O1}$; $d_{\text{D}\cdots\text{A}}$ 3.32 Å, $\angle\text{D}-\text{H}\cdots\text{A}$ 177.54°) interaction. Two different $\text{C}-\text{H}\cdots\text{O}$ ($\text{C5}-\text{H5}\cdots\text{O3}$; $d_{\text{D}\cdots\text{A}}$ 3.50 Å, $\angle\text{D}-\text{H}\cdots\text{A}$ 156.35° and $\text{C8}-\text{H8B}\cdots\text{O4}$; $d_{\text{D}\cdots\text{A}}$ 3.58 Å, $\angle\text{D}-\text{H}\cdots\text{A}$ 159.12°) interactions between the carbonyl oxygen atoms and methylene hydrogen atoms are also observed

in the lattice which further grow the dimension of supramolecular architecture from 1D zigzag chains to 2D sheets as viewed along a -axis. Moreover, three different types of cyclic hydrogen bond motifs, namely $\text{R}_2^2(8)$, $\text{R}_2^2(12)$ and $\text{R}_2^2(11)$ which are formed by the combination of different intermolecular hydrogen bonding interactions [60, 61], are also observed in the lattice. Earlier in the case of *N*-phthaloylglycine, we have demonstrated that the dimeric part can be retained by phenolic guests such as resorcinol [52], such type of assemblies in pyromellitic diimide help in molecular recognition of poly aromatic hydrocarbons [35].

The cocrystal **1a** crystallized in monoclinic $P2_1/n$ space group and its crystallographic asymmetric unit consists of one molecule of **1** and half molecule of bpy that lies on inversion center (Fig. 2). In the structure of **1a**, $-\text{COOH}$ groups of **1** do not enclose cyclic $\text{R}_2^2(8)$ hydrogen bond motif but participate in discrete acceptor $\text{C}-\text{H}\cdots\text{O}$ ($\text{C4}-\text{H4A}\cdots\text{O2}$; $d_{\text{D}\cdots\text{A}}$ 3.58 Å, $\angle\text{D}-\text{H}\cdots\text{A}$ 148.42°) interaction with one of the methylene hydrogen atoms of cyclohexane ring and discrete donor $\text{O}-\text{H}\cdots\text{N}$ ($\text{O1}-\text{H1}\cdots\text{N2}$; $d_{\text{D}\cdots\text{A}}$ 2.74 Å, $\angle\text{D}-\text{H}\cdots\text{A}$ 166.40°) interactions with nitrogen atoms of bpy molecules which makes discrete chains of 32.07 Å length (measured from the center of the aromatic imide ring to the center of the aromatic imide ring) involving two molecules of **1** and one molecules of bpy. The bpy molecules also interact to host molecules via bifurcated $\text{C}-\text{H}\cdots\pi$ ($d_{\text{C31}\cdots\pi}$ 3.61 and $d_{\text{C31}\cdots\pi}$ 3.79 Å) interactions and further connect the discrete chains in another dimension of the lattice. Beside that, the host molecules also assemble in the lattice through $\text{C}-\text{H}\cdots\text{O}$ ($\text{C13}-\text{H13}\cdots\text{O3}$; $d_{\text{D}\cdots\text{A}}$ 3.18 Å, $\angle\text{D}-\text{H}\cdots\text{A}$ 137.61°) and $\text{C}-\text{H}\cdots\pi$ ($d_{\text{C8}\cdots\pi}$ 3.59 Å) interactions to generate 3D network structure of **1a** where repeated tetrameric assemblies of host molecules encapsulate the bpy molecules inside these assemblies as viewed along a axis. Bipyridine or terpyridines are used to make porous building blocks with aromatic polycarboxylic acids [65–67]. We have also shown earlier that different orientations of the weak interactions lead to polymorphic structures in pyridine and quinoline solvates of cyclic imide tethered carboxylic acids [37].

The solvate **1b** crystallized in Triclinic $P\bar{1}$ space group. The asymmetric unit of this has two molecule of **1** with one and half molecule of 1,4-dioxane. The 1,4-dioxane guest molecule which appears as its half in the asymmetric unit, lies on the inversion center and has no interactions with host molecules or another guest molecule (Fig. 3). Another guest molecule interacts with both the host molecules via two different discrete $\text{C}-\text{H}\cdots\text{O}$ ($\text{C12}-\text{H12}\cdots\text{O9}$; $d_{\text{D}\cdots\text{A}}$ 3.28 Å, $\angle\text{D}-\text{H}\cdots\text{A}$ 130.41° and $\text{C20}-\text{H20}\cdots\text{O10}$; $d_{\text{D}\cdots\text{A}}$ 3.48 Å, $\angle\text{D}-\text{H}\cdots\text{A}$ 137.45°) interactions that facilitates again the formation of cyclic $\text{R}_2^2(8)$ hydrogen bond between the two $-\text{COOH}$ groups of two symmetry nonequivalent host molecules by the combination of two $\text{O}-\text{H}\cdots\text{O}$ ($\text{O1}-\text{H1}\cdots\text{O5}$;

Scheme 1 Structure of host **1**, its bpy cocrystal **1a** and its two solvates **1b** and **1c**

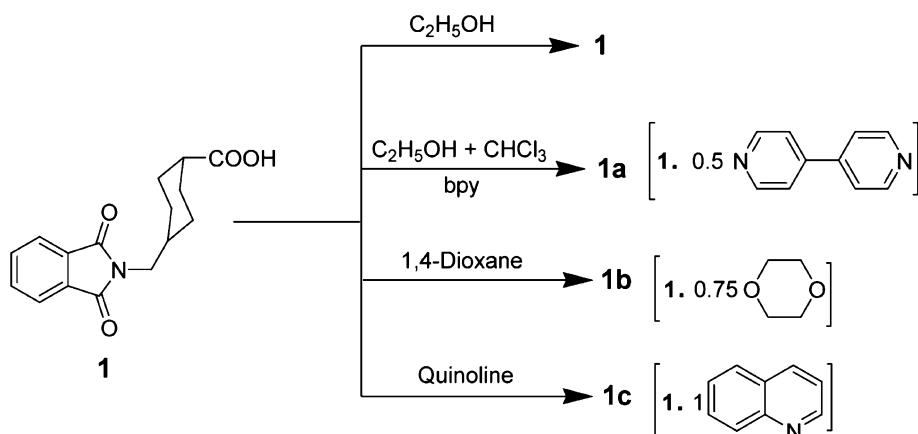
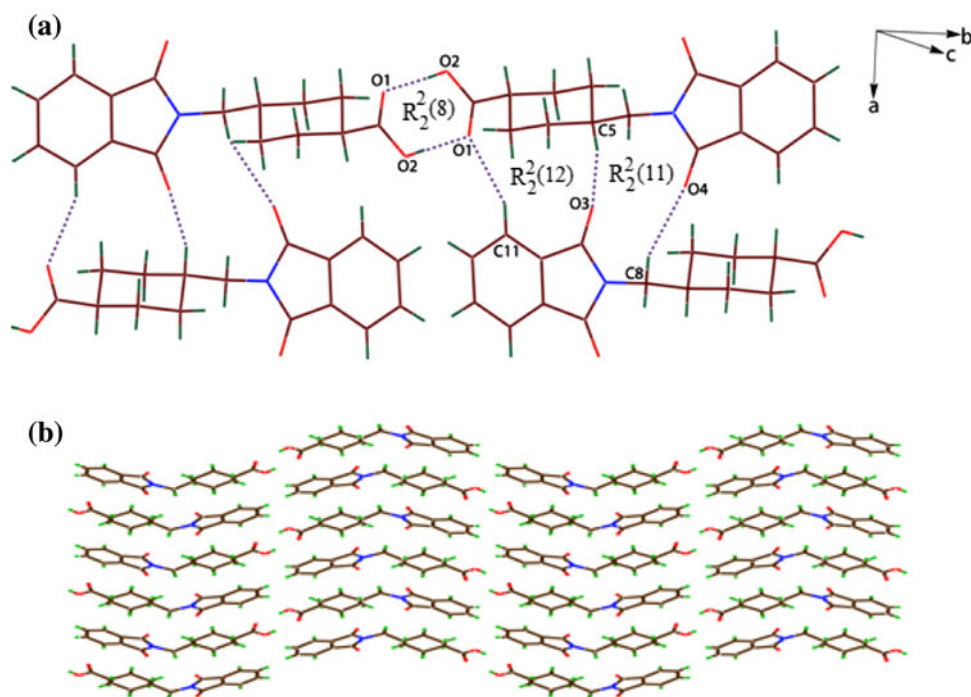


Fig. 1 a A part of crystal structure showing weak interactions in **1**. **b** Crystal packing arrangement showing 2D sheets along *a* axis in the structure of **1**



$d_{D...A}$ 2.66 Å, $\angle D-H...A$ 169.53° and O6–H6...O2; $d_{D...A}$ 2.65 Å, $\angle D-H...A$ 173.79°) interactions. Two cyclic $R_2^2(10)$ motifs also form in the lattice by the combination of two C–H...O (C11–H11...O7; $d_{D...A}$ 3.41 Å, $\angle D-H...A$ 143.36°; C27–H27...O4; $d_{D...A}$ 3.48 Å, $\angle D-H...A$ 146.19° and C14–H14...O8; $d_{D...A}$ 3.49 Å, $\angle D-H...A$ 147.72° and C30–H30...O3; $d_{D...A}$ 3.42 Å, $\angle D-H...A$ 124.86°) interactions exist between the carbonyl oxygen atoms and hydrogen atom of aromatic imide ring of the host. Apart from that, one of the carbonyl oxygen atoms of a host molecule and one of the carboxyl oxygen atoms of another host molecule participate in bifurcated hydrogen bonding and simultaneously interact via two C–H...O (C22–H22...O4; $d_{D...A}$ 3.52 Å, $\angle D-H...A$ 144.09° and C3–H3A...O6; $d_{D...A}$ 3.41 Å, $\angle D-H...A$ 134.56°) interactions making a cyclic $R_2^2(14)$ hydrogen bond motif in the lattice. Moreover, the $\pi\cdots\pi$ interactions between the aromatic imide rings of one of the host molecules are also

observed in the lattice. All these weak interactions found in the crystal lattice of **1b**, result in the construction of 3D host–guest channel structure of **1b** as viewed along *a* axis. The channels of approximate 14 × 11 Å dimensions are filled by guest 1,4-dioxane molecules.

The solvate **1c** crystallized in Orthorhombic $P2_12_12_1$ space group and its crystallographic asymmetric unit consists of one molecule of **1** and one quinoline solvent molecule (Fig. 4). Due to the hierarchy of O–H...N interactions over O–H...O interactions, the cyclic $R_2^2(8)$ hydrogen bond motif is not observed in the crystal lattice of **1c** and the –COOH group of host molecule interacts with quinoline molecule by a combination of O–H...N (O4–H4...N3; $d_{D...A}$ 2.74 Å, $\angle D-H...A$ 177.83°) and C–H...O (C23–H23...O3; $d_{D...A}$ 3.28 Å, $\angle D-H...A$ 125.90°) interactions making a cyclic $R_2^2(7)$ hydrogen bond motif. The quinoline molecule further interact to each other via C–H... π

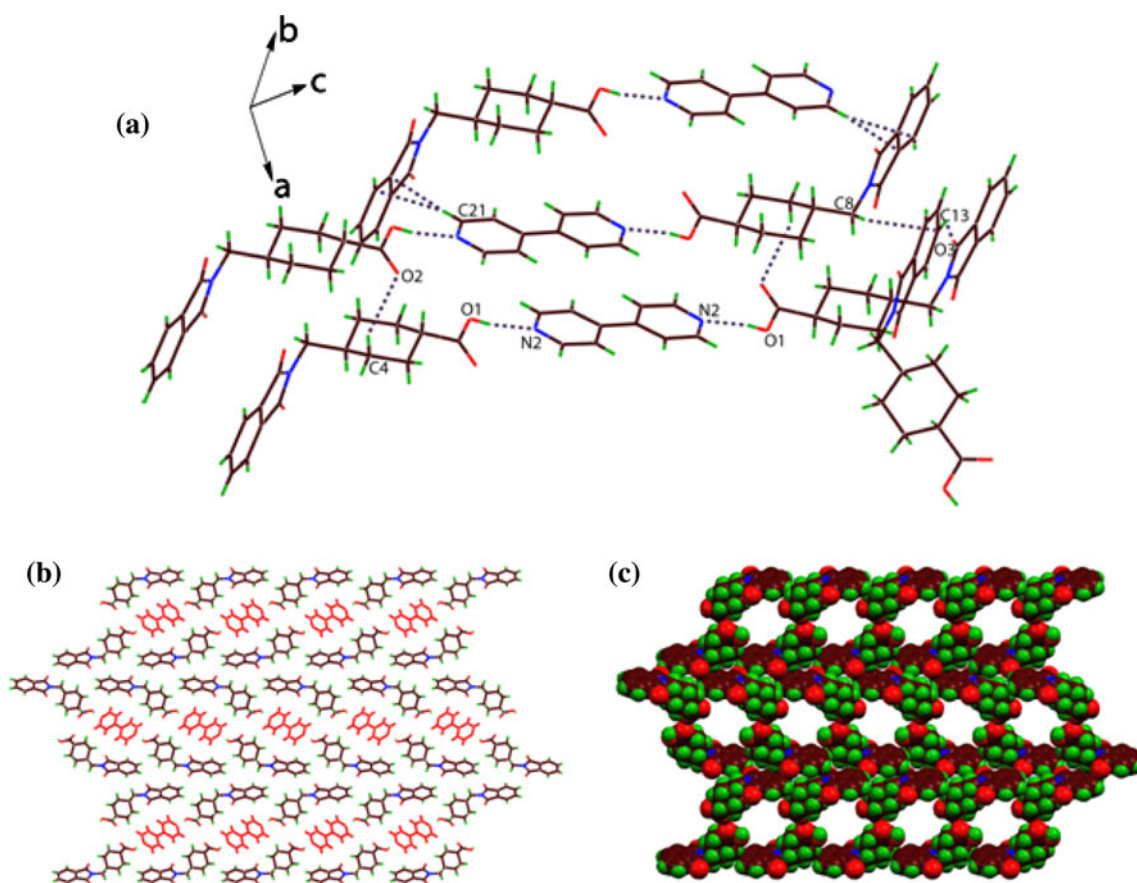


Fig. 2 **a** Weak interactions between the host and guest bpy molecules in the structure of **1a**. **b** 3D tetrameric channel like assemblies of host molecules encapsulating bpy molecules (red) along the *a*-axis. **c** Space filling model after removal of bpy molecules. (Color figure online)

($d_{C19 \dots \pi}$ 3.58 Å) interaction which makes a discrete structure of 27.72 Å length (measured from the center of the aromatic imide ring to the center of the aromatic imide ring) involving two host and two quinoline molecules. The quinoline molecules also interact with the –COOH group and aromatic imide ring of the host molecule via C–H \cdots O (C22–H22 \cdots O3; $d_{D \dots A}$ 3.18 Å, $\angle D-H \dots A$ 131.75°) and C–H $\cdots\pi$ ($d_{C26 \dots \pi}$ 3.62 Å) interactions, respectively, making a 1D host–guest structural arrangement. Beside this, the host molecules also interact to each other via C–H \cdots O (C12–H12 \cdots O2; $d_{D \dots A}$ 3.23 Å, $\angle D-H \dots A$ 137.75°) and C–H $\cdots\pi$ ($d_{C8 \dots \pi}$ 3.62 Å) interactions which assembles the structure as 3D host–guest layered arrangement in which a single layer of quinoline molecules takes the position between the two double layer of host molecules as viewed along *a*-axis.

Thermogravimetric analysis (Figure S1 and S2) of **1b** reveals 18 % weight loss of a three-fourth equivalent of 1,4-dioxane molecule in the temperature range 40–90 °C (calculated: 18.6 %) whereas 30 % weight loss of one equivalent of quinoline molecule occurs from **1c** in the temperature range 75–150 °C (calculated: 31 %). Powder X-ray diffraction (PXRD) patterns for host **1** and its different host–guest crystalline forms, **1a**, **1b** and **1c** are

differed to each other (Fig. 5). The differences observed in the position and intensity of the diffraction peaks of these various crystalline forms are due to the presence of solvent or other addition molecules in the crystal lattice of host. The peaks obtained in the PXRD patterns of **1** and its other forms correlate well with the simulated peaks of single crystal X-ray structures (Figure S3–S6).

The crystals of two different solvates of **2**, namely **2a** and **2b**, in 1:1 host to guest ratio are obtained from DMF and quinoline solution of **2**, respectively, and their structures are also determined (Scheme 2).

Crystal structure analysis revealed that solvate **2a** crystallized in triclinic $P\bar{1}$ space group, included one molecule of **2** and one molecule of solvent water in its crystallographic asymmetric unit (Fig. 6). In the crystal lattice, cyclic O–H \cdots O interactions between the –COOH groups of host molecules are absent due to the presence of water molecules which are engaged in discrete O–H \cdots O hydrogen bonds with host molecules and act as both donor and acceptor. The oxygen atom of water molecule involves bifurcated acceptor hydrogen bonding via two different interactions, namely, O–H \cdots O (O1–H1 \cdots O5; $d_{D \dots A}$ 2.66 Å, $\angle D-H \dots A$ 172.57°) and C–H \cdots O (C16–H16 \cdots O5; $d_{D \dots A}$

Fig. 3 **a** Weak interactions in the host–guest assembly of **1b**. **b** Channel formation in the assembly of host and 1,4-dioxane molecules (along *a* axis). **c** Space filling model after removal of 1,4-dioxane molecules residing inside the channels

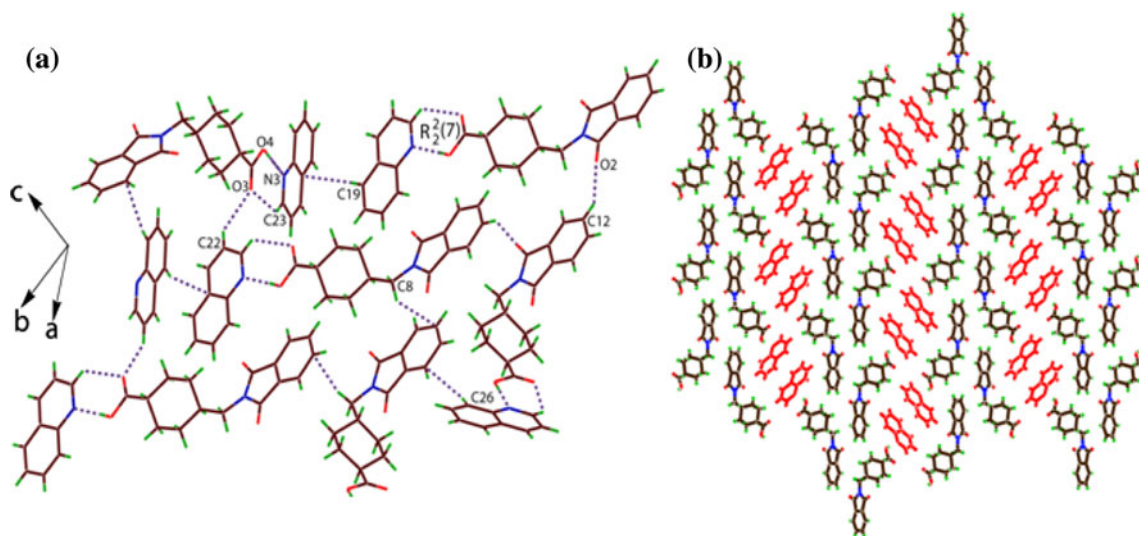
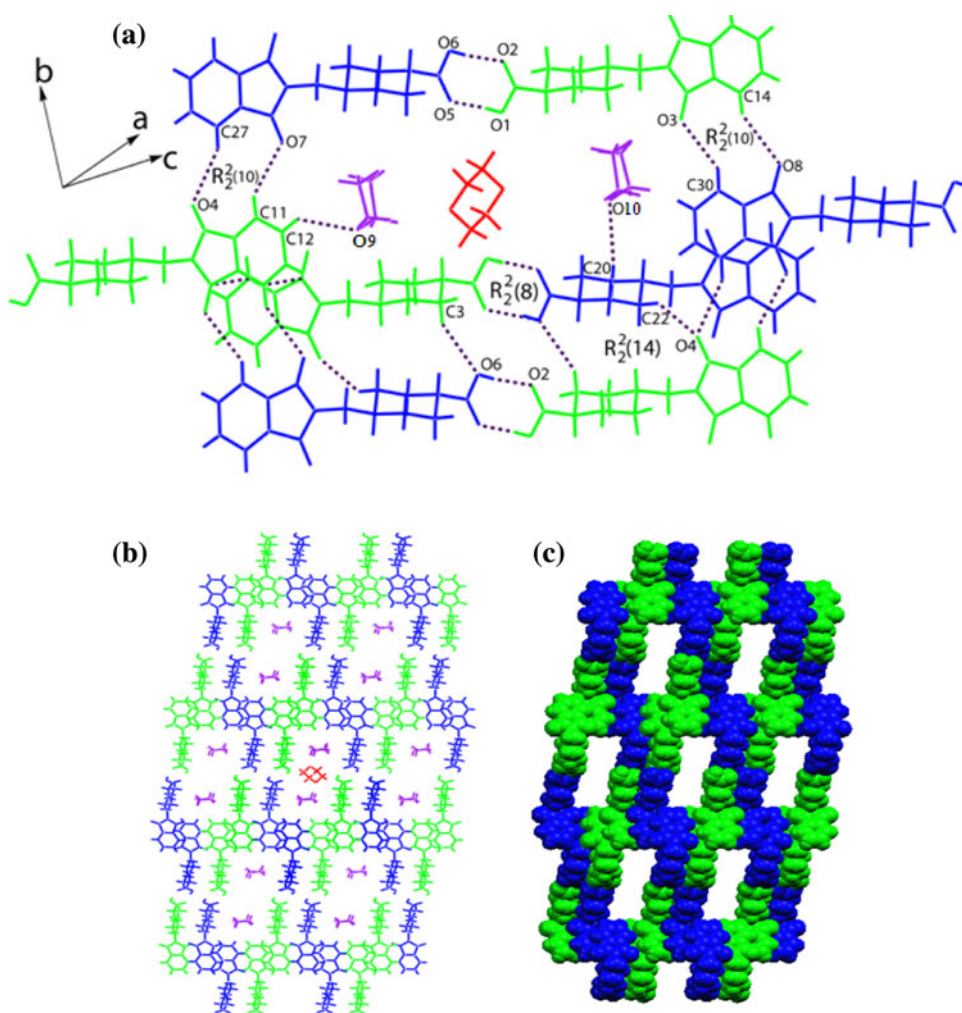


Fig. 4 **a** Weak interactions between the host and quinoline molecules in **1c**. **b** Crystal packing of **1c**, showing the arrangement of host and quinoline molecules in the crystal lattice (along *a* axis)

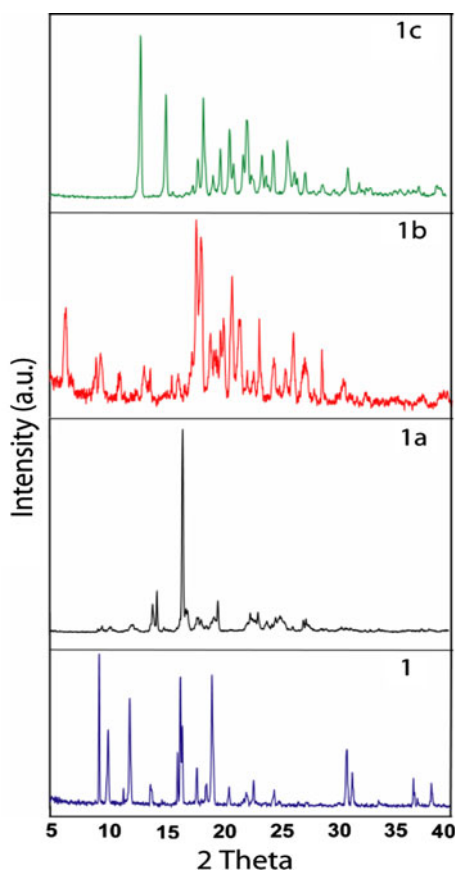
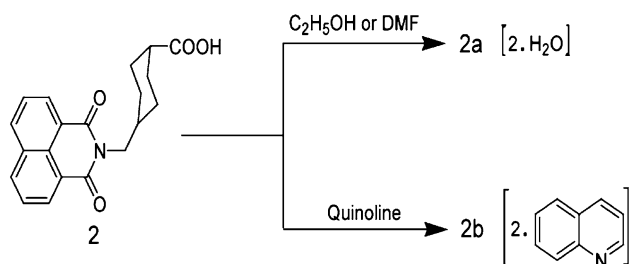


Fig. 5 PXRD patterns of **1**, **1a**, **1b** and **1c**



Scheme 2 Structure of host **2** and its two solvates

3.48 Å, $\angle\text{D}\cdots\text{H}\cdots\text{A}$ 144.39°) interactions and both the hydrogen atoms engage in donor hydrogen bonding with two carbonyl oxygen atoms of host molecule through O–H \cdots O (O5–H5A \cdots O3; $d_{\text{D}\cdots\text{A}}$ 2.83 Å, $\angle\text{D}\cdots\text{H}\cdots\text{A}$ 171.43° and O1–H1 \cdots O5; $d_{\text{D}\cdots\text{A}}$ 2.79 Å, $\angle\text{D}\cdots\text{H}\cdots\text{A}$ 168.96°) interactions making two different cyclic $R_4^4(26)$ hydrogen bond motifs in the lattice. The host molecules also interact with each other via C–H \cdots O (C13–H13 \cdots O2; $d_{\text{D}\cdots\text{A}}$ 3.23 Å, $\angle\text{D}\cdots\text{H}\cdots\text{A}$ 149.53°) interaction which overall makes a 2D channel like host–guest network of **2a** in the crystal lattice as viewed along *a*-axis.

The solvate **2b** crystallized in monoclinic $P2_1/c$ space group, included one molecule of **2** and one molecule of

solvent quinoline in its crystallographic asymmetric unit (Fig. 7). Similar to quinoline solvate **1c**, the –COOH groups of the host molecules do not enclose cyclic O–H \cdots O hydrogen bond formation and interact apparently with guest quinoline molecules via both discrete donor O–H \cdots N (O3–H3 \cdots N2; $d_{\text{D}\cdots\text{A}}$ 2.67 Å, $\angle\text{D}\cdots\text{H}\cdots\text{A}$ 171.88°) and discrete acceptor C–H \cdots O (C24–H24 \cdots O3; $d_{\text{D}\cdots\text{A}}$ 3.46 Å, $\angle\text{D}\cdots\text{H}\cdots\text{A}$ 169.82°) interactions forming cyclic $R_4^4(14)$ hydrogen bond motif in the lattice which involves two quinoline and two host molecules. Another cyclic $R_3^3(12)$ hydrogen bond motif is also formed in the lattice by the combinations of three different interactions, namely host–guest O3–H3 \cdots N2, host–guest C30–H30 \cdots O2 ($d_{\text{D}\cdots\text{A}}$ 3.18 Å, $\angle\text{D}\cdots\text{H}\cdots\text{A}$ 131.45°) and host–host C8–H8 \cdots O4 ($d_{\text{D}\cdots\text{A}}$ 3.33 Å, $\angle\text{D}\cdots\text{H}\cdots\text{A}$ 155.09°) interactions, which involves one quinoline and two host molecules. The host molecules also assemble in the lattice through C–H $\cdots\pi$ ($d_{\text{C16}\cdots\pi}$ 3.60 Å) interactions experienced between the hydrogen atoms of cyclohexane ring and aromatic imide ring. No weak interactions among the quinoline molecules are observed in the lattice of **2b**. All these host–host and host–guest interactions result in the construction of repeated 3D hexameric assemblies of host molecules allowing the formation of large voids in the lattice which are filled by quinoline molecules as viewed along *a* axis. The quinoline molecules generally form strong cyclic $R_2^2(7)$ and $R_2^2(8)$ hydrogen bonds with –COOH functional groups in the lattice [37, 38]. This is valid in the case of solvate **1c**. Exception is observed that quinoline molecules are held with the host molecules through discrete donor–acceptor interactions in the lattice of **2b**.

Thermogravimetric studies on two different solvates of **2** (Figure S3 and S4) show that solvate **2a** loses 4.8 % weight in the temperature range 97–154 °C which corresponds to the loss of one equivalent of water molecule (calculated: 5.2 %). Another solvate **2b** also shows 22 % weight loss of one equivalent of quinoline molecule in the temperature range 60–145 °C (calculated: 27.6 %). Significant differences are observed in the PXRD patterns of guest free crystalline form of host **2** and its two solvates, **2a** and **2b**, which are crystallized in different space groups (Fig. 8). These differences can be accounted for the inclusion of different solvents in the crystal lattice of host. PXRD patterns of all three different crystalline materials are in good correlation with the simulated patterns of single crystal X-ray structures determined at 298 K.

Conclusions

The role of weak interactions between the hosts and guests (solvents or other additional molecules) in the formation of different cyclic hydrogen bond motifs in different structures of hosts **1** and **2** is discussed. The structural features of **1** and **1b** reveals the formation of cyclic $R_2^2(8)$ motifs by intermolecular

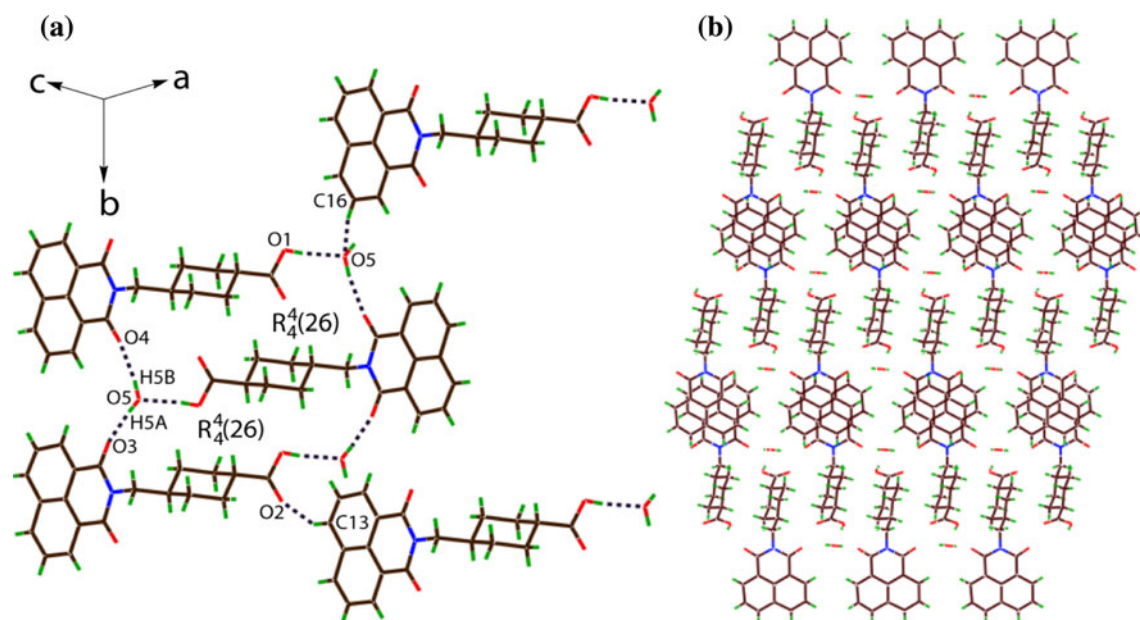


Fig. 6 **a** A part of crystal structure showing host-guest weak interactions in **2a**. **b** Crystal packing arrangement showing the channel like structure of **2a**

acid...acid interactions whereas the structures of **1a** and **1c** are devoid of these $R_2^2(8)$ interactions and are governed by discrete O-H...N interactions or cyclic $R_2^2(7)$ interactions. Formation of repeated 3D tetrameric assemblies of host molecules occurs in **1a** which encapsulate the additional bpy molecules inside themselves whereas 3D channels of approximate $14 \times 11 \text{ \AA}$ dimension accommodate the guest 1,4-dioxane molecules in the crystal lattice of **1b**. In the structure of **1b**, two symmetry nonequivalent molecules of host are also responsible for the formation of three types of cyclic hydrogen bond motifs, namely, $R_2^2(8)$, $R_2^2(10)$ and $R_2^2(14)$, through different weak interactions. The discrete O-H...O interactions observed between the water and host molecules are sufficient enable to cleave the dimeric assembly of carboxylic acid moiety in the structure of **2a** and these water molecules occupy the positions inside the 2D channels like network of host molecules. Instead of making conventionally observed cyclic $R_2^2(7)$ or $R_2^2(8)$ hydrogen bond motifs, the quinoline molecules are held in the repeated hexameric assemblies by discrete O-H...N and C-H...O interactions in the structure of **2b**, which allows the creation of large solvent voids.

Experimental section

General

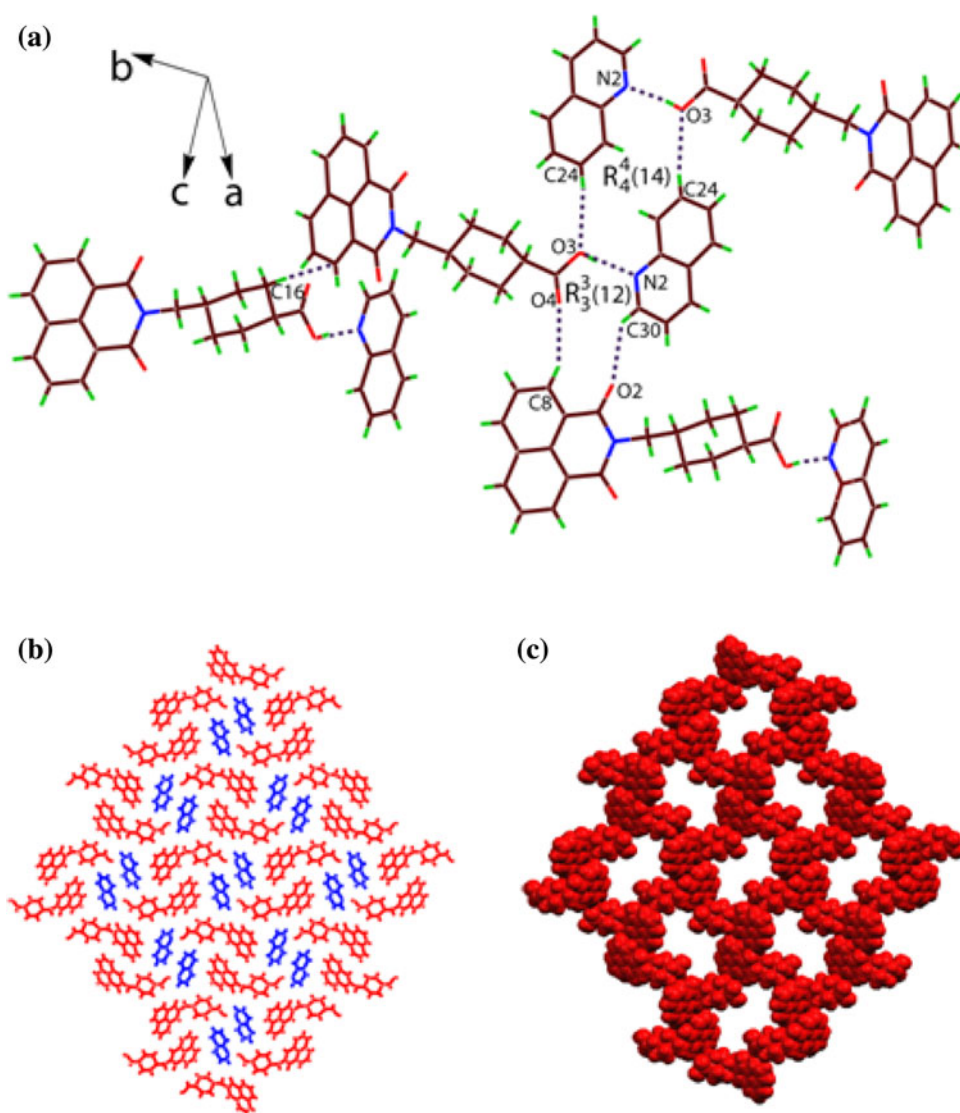
All reagents and solvents were obtained from commercial sources. The IR spectra were recorded on a Perkin-Elmer-Spectrum One FT-IR spectrometer with KBr disks in the range $4,000\text{--}400 \text{ cm}^{-1}$. The ^1H NMR and ^{13}C NMR spectra

were recorded using a Varian Mercury plus 400 MHz instrument. Chemical shifts were reported in parts per million (ppm) relative to internal TMS (0 ppm). Electrospray ionization mass (ESI-MS) spectra were recorded on a Waters (Micromass MS Technologies) Q-ToF Premier mass spectrometer. PXRD data were collected on a Bruker D2 diffractometer in Bragg-Brentano $\theta\text{--}\theta$ geometry with $\text{Cu K}\alpha$ radiation ($\lambda = 1.5418 \text{ \AA}$) on a glass surface of an air-dried sample using a secondary curved graphite monochromator. Diffraction patterns were collected over a 2θ range of $5\text{--}50^\circ$ at a scan rate of 2° min^{-1} . Thermogravimetric analyses (TGA) were performed on a Mettler Toledo TGA/SDTA 851e module. Samples were placed in open alumina pans in the temperature range $25\text{--}300 \text{ }^\circ\text{C}$ and were purged with a stream of dry N_2 flowing at 100 mL min^{-1} .

Structure determination

The X-ray single crystal diffraction data were collected at 296 K with $\text{MoK}\alpha$ radiation ($\lambda = 0.71073 \text{ \AA}$) using a Bruker Nonius SMART CCD diffractometer equipped with a graphite monochromator. The SMART software was used for data collection and also for indexing the reflections and determining the unit cell parameters; the collected data were integrated using SAINT software. The structures were solved by direct methods and refined by full-matrix least-squares calculations using SHELXTL software [68]. All the non-H atoms were refined in the anisotropic approximation against F^2 of all reflections. The H-atoms, except those attached to nitrogen and oxygen atoms were placed at their calculated positions and refined in the isotropic

Fig. 7 **a** Host–guest weak interactions in a part of crystal structure of **2b**. **b** 3D hexameric assemblies of host molecules (red) encapsulating quinoline molecules (blue) along the *a* axis. **c** Space filling model after removal of the quinoline molecules inside the voids. (Color figure online)



approximation; those attached to nitrogen and oxygen were located in the difference Fourier maps, and refined with isotropic displacement coefficients. Crystallographic data collection was done at room temperature and the data are tabulated in Table 1. The CCDC numbers of the compounds **1**, **1a**, **1b**, **1c**, **2a** and **2b** are 826469–826474.

Synthesis and characterization of compounds and their solvates

Compound **1**

A solution of phthalic anhydride (0.740 g, 5 mmol) and trans-4-(aminomethyl)cyclohexanecarboxylic acid (0.785 g, 5 mmol) in acetic acid (20 mL) was refluxed for 3 h. The reaction mixture was cooled to room temperature, poured into ice cooled water (50 mL) and stirred for 15 min. A white colored crystalline product was obtained. This was filtered and

dried in open air. The crystals of solvent free host **1** were obtained by recrystallizing it from dry ethanol in a sealed test tube. Yield: 85 %; IR (KBr, cm^{-1}): 3406 (w), 2915 (m), 2854 (m), 2528 (w), 1769 (w), 1712 (s), 1596 (s), 1538 (w), 1433 (m), 1399 (s), 1360 (m), 1331 (m), 1304 (m), 1249 (m), 1223 (m), 1197 (s), 1158 (m), 1061 (m), 983 (w), 805 (m), 772 (m). $^1\text{H NMR}$ (400 MHz, CDCl_3): 7.82 (dd, 2H, $J = 2.8$ Hz), 7.69 (dd, 2H, $J = 3.2$ Hz), 3.52 (d, 2H, $J = 6.8$ Hz), 2.24 (t, 1H, $J = 12.0$ Hz), 2.00 (d, 2H, $J = 10.8$ Hz), 1.78 (d, 3H, $J = 6.8$ Hz), 1.37 (q, 2H, $J = 8.4$ Hz), 1.07 (q, 2H, $J = 10.4$ Hz). $^{13}\text{C NMR}$ (CDCl_3): 168.9, 150.4, 145.9, 134.1, 132.2, 123.4, 121.8, 43.9, 43.2, 36.6, 30.0, 28.5. ESI-MS: 288.156 [$\text{M} + \text{H}^+$].

Compound **1a**

The solvent free crystals of **1** (0.287 g, 1 mmol) were dissolved again in dry ethanol and a pre prepared solution

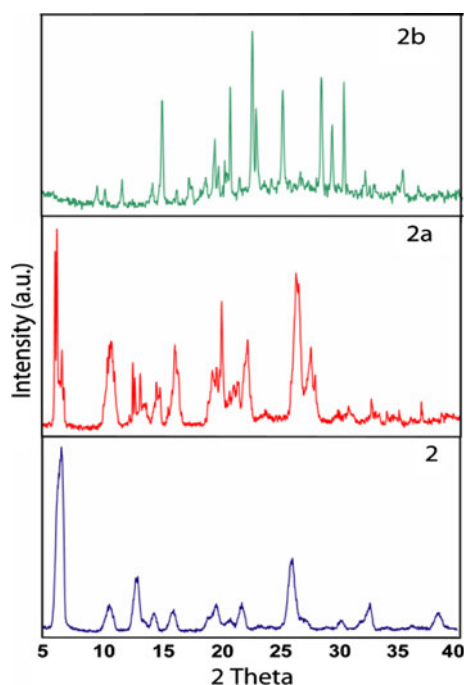


Fig. 8 PXRD patterns of **2**, **2a**, and **2b**

of bpy (0.078 g, 0.5 mmol) in dry chloroform was layered over the ethanol solution in a sealed test tube. Colorless needle shape crystals of **1a** were obtained after five days. IR (KBr, cm^{-1}): 3463 (w), 2932(m), 2856 (m), 1773 (w), 1705 (s), 1400 (m), 1366 (m), 1336 (m), 1263 (m), 1211 (m), 1189 (w), 1153 (w), 1054 (m), 951 (w), 933 (w), 719 (m), 713 (m). ^1H NMR (400 MHz, CDCl_3): 8.72 (d, 2H, $J = 4.8$ Hz), 7.82 (dd, 2H, $J = 3.2$ Hz), 7.68 (dd, 2H, $J = 4.0$ Hz), 7.52 (d, 2H, $J = 6.0$ Hz), 3.52 (d, 2H, $J = 6.8$ Hz), 2.26 (t, 1H, $J = 12.8$ Hz), 2.02 (d, 2H, $J = 11.6$ Hz), 1.80 (d, 3H, $J = 10.0$ Hz), 1.40 (q, 2H, $J = 10.4$ Hz), 1.08 (q, 2H, $J = 8.8$ Hz).

Compound **1b**

The crystals of solvate **1b** were obtained as white blocks from a solution of compound **1** in 1,4-dioxane. IR (KBr, cm^{-1}): 3456 (w), 2924 (m), 2859 (m), 1770 (w), 1709 (s), 1415 (m), 1390 (m), 1366 (m), 1336 (m), 1255 (m), 1211 (m), 1196 (w), 1173 (w), 1054 (m), 986 (w), 950 (w), 930 (w), 770 (m), 722 (m). ^1H NMR (400 MHz, CDCl_3): 8.71 (d, 6H, $J = 4.4$ Hz), 7.81 (m, 2H), 7.67 (m, 2H), 7.53 (d, 6H, $J = 4.4$ Hz), 3.51 (d, 2H, $J = 6.8$ Hz), 2.25 (t, 1H, $J = 12.0$ Hz), 2.00 (d, 2H, $J = 10.8$ Hz), 1.78 (d, 3H, $J = 10.8$ Hz), 1.37 (q, 2H, $J = 12.4$ Hz), 1.07 (q, 2H, $J = 11.2$ Hz).

Compound **1c**

The solvate **1c** was crystallized as brown colored blocks from the quinoline solution of compound **1**. IR (KBr,

cm^{-1}): 3459 (w), 2932 (m), 2849 (m), 2528 (w), 1925 (w), 1770 (w), 1713 (s), 1431 (w), 1396 (m), 1357 (m), 1329 (m), 1305 (m), 1251 (m), 1222 (w), 1209 (m), 1058 (m), 984 (w), 950 (w), 927(w), 816 (m), 788 (w), 722 (m). ^1H NMR (400 MHz, CDCl_3): 8.92 (d, 2H, $J = 3.2$ Hz), 8.16 (dd, 2H, $J = 8.0$ Hz), 7.81 (m, 2H), 7.70 (m, 2H), 7.54 (t, 1H, $J = 7.6$ Hz), 7.40 (dd, 2H, $J = 4.0$ Hz), 3.52 (d, 2H, $J = 6.4$ Hz), 2.26 (t, 1H, $J = 12.0$ Hz), 2.04 (d, 2H, $J = 12.4$ Hz), 1.78 (d, 3H, $J = 10.8$ Hz), 1.40 (q, 2H, $J = 12.0$ Hz), 1.06 (q, 2H, $J = 12.4$ Hz).

Compound **2**

A solution of 1,8-naphthalic anhydride (0.990 g, 5 mmol) and *trans*-4-(aminomethyl)cyclohexanecarboxylic acid (0.785 g, 5 mmol) in *N,N*-dimethylformamide (15 mL) was refluxed for 5 h. The reaction mixture was cooled to room temperature, poured into ice cooled water (30 mL) and stirred for 15 min. A brown colored precipitate of the product was formed, which was filtered and air dried. Yield: 78 %; IR (KBr, cm^{-1}): 3501 (s), 2946 (s), 2855 (m), 1725 (s), 1695 (s), 1651 (s), 1590 (m), 1442 (w), 1389 (w), 1354 (m), 1316 (w), 1255 (m), 1237 (m), 1198 (m), 1176 (m), 1074 (w), 1030 (w), 973 (w), 935 (w), 776 (m). ^1H NMR (400 MHz, CDCl_3): 8.57 (d, 2H, $J = 7.2$ Hz), 8.19 (d, 2H, $J = 8.0$ Hz), 7.73 (d, 2H, $J = 7.2$ Hz), 4.05 (d, 2H, $J = 6.8$ Hz), 2.26 (t, 1H, $J = 9.2$ Hz), 2.00 (d, 2H, $J = 13.2$ Hz), 1.82 (d, 3H, $J = 14.0$ Hz), 1.34 (q, 2H, $J = 12.0$ Hz), 1.18 (q, 2H, $J = 11.2$ Hz). ^{13}C NMR (CDCl_3): 164.8, 134.2, 131.6, 127.2, 122.8, 45.9, 43.01, 36.2, 30.1, 28.4. ESI-MS: 338.185 [$\text{M} + \text{H}^+$].

Compound **2a**

The crystals of the solvate **2a** were obtained from a solution of compound **2** from any of the solvents like ethanol, isopropanol, t-butanol, *N,N*-dimethylformamide, dimethylsulphoxide and pyridine as brown colored blocks. IR (KBr, cm^{-1}): 3504 (s), 2946 (s), 2855 (m), 1724 (s), 1695 (s), 1650 (s), 1621 (s), 1589 (s), 1441 (w), 1346 (m), 1316 (m), 1254 (m), 1237 (m), 1198 (m), 1176 (m), 1074 (w), 917 (w), 776 (w). ^1H NMR (400 MHz, CDCl_3): 8.57 (d, 2H, $J = 7.6$ Hz), 8.19 (d, 2H, $J = 8.4$ Hz), 7.73 (d, 2H, $J = 8.0$ Hz), 4.05 (d, 2H, $J = 7.2$ Hz), 2.26 (t, 1H, $J = 12.4$ Hz), 2.00 (d, 2H, $J = 11.2$ Hz), 1.82 (d, 3H, $J = 12.8$ Hz), 1.34 (q, 2H, $J = 10.4$ Hz), 1.18 (q, 2H, $J = 11.2$ Hz).

Compound **2b**

The solvate **2b** was obtained by crystallization of compound **2** from quinoline solution as brown block crystals. IR (KBr, cm^{-1}): 3503 (w), 2925 (m), 2851 (m), 2485 (w),

Table 1 Crystallographic parameters of **1**, **1a**, **1b**, **1c**, **2a** and **2b**

Compound No.	1	1a	1b	1c	2a	2b
Formulae	C ₁₆ H ₁₇ N O ₄	C ₂₁ H ₂₁ N ₂ O ₄	C ₃₈ H ₄₆ N ₂ O ₁₁	C ₂₅ H ₂₄ N ₂ O ₄	C ₂₀ H ₂₁ N O ₅	C ₂₉ H ₂₆ N ₂ O ₄
Formula. wt.	287.31	365.40	706.77	416.46	355.38	466.52
Crystal system	Monoclinic	Monoclinic	Triclinic	Orthorhombic	Triclinic	Monoclinic
Space group	P2 ₁ /c	P2 ₁ /n	P $\bar{1}$	P2 ₁ 2 ₁ 2 ₁	P $\bar{1}$	P2 ₁ /c
<i>a</i> (Å)	5.5389(9)	5.3895(3)	6.9998(7)	5.4464(4)	7.0784(4)	5.12940(10)
<i>b</i> (Å)	26.406(4)	11.4669(6)	13.6084(14)	11.6278(8)	9.0908(6)	18.4728(4)
<i>c</i> (Å)	10.8187(15)	29.4655(16)	19.931(2)	33.471(2)	14.4330(8)	25.1209(5)
α (°)	90.00	90.00	74.897(7)	90.00	101.630(4)	90.00
β (°)	116.329(9)	93.998(3)	84.667(7)	90.00	99.886(4)	91.5870(10)
γ (°)	90.00	90.00	80.376(7)	90.00	103.335(4)	90.00
<i>V</i> (Å ³)	1418.2(4)	1816.56(17)	1804.8(3)	2119.7(3)	861.64(9)	1593.12(9)
<i>Z</i>	4	4	2	4	2	4
Density (Mg ⁻³)	1.346	1.336	1.301	1.305	1.370	1.302
Abs. Coeff. (mm ⁻¹)	0.097	0.093	0.096	0.089	0.099	0.087
<i>F</i> (000)	608	772	752	880	376	984
Total no. of reflections	7,729	24,847	16,749	16,715	10,403	18,030
Reflections, <i>I</i> > 2σ(<i>I</i>)	1,428	2,986	3,339	2,473	1,794	1,860
Max. 2θ (°)	50.00	56.76	45.06	49.98	50.00	44.12
Ranges (<i>h</i> , <i>k</i> , <i>l</i>)	−6 ≤ <i>h</i> ≤ 6 −31 ≤ <i>k</i> ≤ 27 −11 ≤ <i>l</i> ≤ 11	−7 ≤ <i>h</i> ≤ 7 −12 ≤ <i>k</i> ≤ 15 −39 ≤ <i>l</i> ≤ 32	−7 ≤ <i>h</i> ≤ 7 −14 ≤ <i>k</i> ≤ 14 −21 ≤ <i>l</i> ≤ 21	−6 ≤ <i>h</i> ≤ 6 −13 ≤ <i>k</i> ≤ 13 −39 ≤ <i>l</i> ≤ 35	−8 ≤ <i>h</i> ≤ 8 −10 ≤ <i>k</i> ≤ 10 −17 ≤ <i>l</i> ≤ 17	−5 ≤ <i>h</i> ≤ 5 −19 ≤ <i>k</i> ≤ 19 −26 ≤ <i>l</i> ≤ 26
Completeness to 2θ (%)	81.9	99.5	98.9	99.2	99.5	99.5
Data/restraints/parameters	2,048/0/190	4,525/1/245	4,694/0/462	3,677/0/281	3,019/0/244	2,943/0/317
Goof (<i>F</i> ²)	1.045	1.058	1.078	1.047	1.081	0.891
<i>R</i> indices [<i>I</i> > 2σ(<i>I</i>)]	0.0663	0.0543	0.0689	0.0524	0.0589	0.0466
<i>R</i> indices (all data)	0.0831	0.0867	0.0930	0.0854	0.0960	0.0718

1901 (w), 1698 (s), 1661 (s), 1627 (m), 1591 (m), 1505 (w), 1427 (w), 1342 (m), 1254 (m), 1233 (m), 1207 (m), 1176 (m), 1073 (w), 1028 (w), 811 (m), 782 (m). ¹HNMR (400 MHz, CDCl₃): 8.91 (d, 2H, *J* = 4.4 Hz), 8.58 (d, 2H, *J* = 7.2 Hz), 8.19 (d, 2H, *J* = 8.4 Hz), 7.87 (t, 1H, *J* = 6.8 Hz), 7.73 (t, 2H, *J* = 8.0 Hz), 7.54 (t, 1H, *J* = 6.8 Hz), 7.40 (dd, 2H, *J* = 4.4 Hz), 4.06 (d, 2H, *J* = 10.4 Hz), 2.27 (t, 1H, *J* = 8.4 Hz), 2.02 (d, 2H, *J* = 12.8 Hz), 1.82 (d, 3H, *J* = 12.4 Hz), 1.36 (q, 2H, *J* = 12.8 Hz), 1.19 (q, 2H, *J* = 12.0 Hz).

Acknowledgments The authors thank Department of Science and Technology, New Delhi (India) for financial support. One of the authors DS is thankful to Council of Scientific and Industrial Research, New Delhi (India) for senior research fellowship.

References

- Desiraju, G.R.: Supramolecular synthons in crystal engineering: a new organic synthesis. *Angew. Chem. Int. Ed.* **34**, 2311 (1995)
- Steiner, T.: The hydrogen bond in the solid state. *Angew. Chem. Int. Ed.* **41**, 48 (2002)
- Huang, K.-S., Britton, O., Bryn, S.R., Etter, M.C.J.: A novel class of phenol–pyridine co-crystals for second harmonic generation. *Mater. Chem.* **7**, 713 (1997)
- Gavezzotti, A.: Are crystal structures predictable? *Acc. Chem. Res.* **27**, 309 (1994)
- Almarsson, O., Zaworotko, M. J.: Crystal engineering of the composition of pharmaceutical phases. Do pharmaceutical co-crystals represent a new path to improved medicines? *Chem. Commun.* 1889–1896 (2004)
- Moulton, B., Zaworotko, M.J.: From molecules to crystal engineering: supramolecular isomerism and polymorphism in network solids. *Chem. Rev.* **101**, 1629 (2001)
- Dunitz, J. D.: Are crystal structures predictable? *Chem. Commun.* 545–548 (2003)
- Wuest, J. D.: Engineering crystals by the strategy of molecular tectonics. *Chem. Commun.* 5830–5837 (2005)
- Nishio, M.: CH/π hydrogen bonds in crystals. *CrystEngComm* **6**, 130 (2004)
- Hosseini, M.W.: Reflexion on molecular tectonics. *CrystEngComm* **6**, 318 (2004)
- Byrn, S.R.: *Solid-State Chemistry of Drugs*. Academic, New York (1982)
- Desiraju, G.R.: Crystal gazing: structure prediction and polymorphism. *Science* **278**, 404 (1996)
- Jetti, R.K.R., Boese, R., Sarma, J.A.R.P., Reddy, L.S.R., Vishweshwar, P., Desiraju, G.R.: Cocrystallization with acetylene:

- molecular complexes with acetone and dimethyl sulfoxide. *Angew. Chem. Int. Ed.* **42**, 1963 (2003)
14. Yu, L.J.: Nucleation of one polymorph by another. *Am. Chem. Soc.* **125**, 6380 (2003)
 15. Duntiz, J.D., Bernstein, J.: Disappearing polymorphs. *Acc. Chem. Res.* **28**, 193 (1995)
 16. Hennigar, T.L., MacQuarrie, D.C., Losier, P., Rogers, R.D., Zaworotko, M.J.: Supramolecular isomerism in coordination polymers: manifestations of ligand flexibility in $[\text{Co}(\text{NO}_3)_2(1,2\text{-bis}(4\text{-pyridyl)ethane})_{1.5}]_n$. *Angew. Chem. Int. Ed.* **36**, 972 (1997)
 17. Bhatt, P. M.; Ravindra, N. V.; Banerjee, R.; Desiraju, G. R.: Saccharin as a salt former. Enhanced solubilities of saccharinates of active pharmaceutical ingredients. *Chem. Commun.* 1073–1075 (2005)
 18. Visheswar, A.P., McMahon, J.A., Bis, J.A., Zaworotko, M.J.J.: Pharmaceutical co-crystals. *Pharm. Sci.* **95**, 499 (2006)
 19. Morissette, S.L., Almarsson, O., Peterson, M.L., Remenar, J.F., Read, M.J., Lemmo, A.V., Ellis, S., Cima, M.J., Gardner, C.R.: Crystals and solvates of pharmaceutical solids. *Adv. Drug Deliv. Rev.* **56**, 275 (2004)
 20. Weyna, D.R., Shattock, T., Visweshwar, P., Zaworotko, M.J.: Synthesis and structural characterization of cocrystals and pharmaceutical cocrystals: mechanochemistry vs slow evaporation from solution. *Cryst. Growth Des.* **9**, 1106 (2009)
 21. Halder, G.J., Kepert, C.J., Moubaraki, B., Murray, K.S., Cashion, J.D.: Guest-dependent spin crossover in a nanoporous molecular framework material. *Science* **298**, 1762 (2002)
 22. Kitaura, R., Seki, K., Akiyama, G., Kitagawa, S.: Porous coordination-polymer crystals with gated channels specific for supercritical gases. *Angew. Chem. Int. Ed.* **42**, 428 (2003)
 23. Yaghi, O.M., O'K, M., Ockwig, N.W., Chae, H.K., Eddaoudi, M., Kim, J.: Reticular synthesis and the design of new materials. *Nature* **423**, 705 (2003)
 24. Mahender, J.Y., Dewal, B., Shimizu, L.S.J.: Self-assembling bisurea macrocycles used as an organic zeolite for a highly stereoselective photodimerization of 2-cyclohexenone. *Am. Chem. Soc.* **128**, 8122 (2006)
 25. Rebek, J., Askew, B., Ballester, P., Buhr, C., Jones, S., Nemeth, D., Williams, K.J.: Structure of FK506, a novel immunosuppressant isolated from streptomyces. *Am. Chem. Soc.* **109**, 5033 (1987)
 26. Seneque, O., Rager, M.-N., Giorgi, M., Reinaud, O.J.: Calix[6]arenes and zinc: biomimetic receptors for neutral molecules. *Am. Chem. Soc.* **122**, 6183 (2000)
 27. Fiedler, D., Leung, D.H., Bergman, R.G., Raymond, K.N.: Selective molecular recognition, C–H bond activation, and catalysis in nanoscale reaction vessels. *Acc. Chem. Res.* **38**, 349 (2005)
 28. Yoshizawa, M., Klosterman, J.K., Fujita, M.: Functional molecular flasks: new properties and reactions within discrete, self-assembled hosts. *Angew. Chem. Int. Ed.* **48**, 3418 (2009)
 29. Colquhoun, H.M., Williams, D.J., Zhu, Z.J.: Macrocyclic aromatic ether-imide-sulfones: versatile supramolecular receptors with extreme thermochemical and oxidative stability. *Am. Chem. Soc.* **124**, 13346 (2002)
 30. Cheney, M.L., McManus, G.J., Perman, J.A., Wang, Z., Zaworotko, M.J.: The role of cocrystals in solid-state synthesis: cocrystal-controlled solid-state synthesis of imides. *Cryst. Growth Des.* **7**, 616 (2007)
 31. Degenhardt III, C.; Shortell, D. B.; Adams, R. D.; Shimizu, K. D.: Synthesis and structural characterization of adaptable shape-persistent building blocks. *Chem. Comm.* 929–930 (2000)
 32. Degenhardt, C.F., Lavin, J.M., Smith, M.D., Shimizu, K.D.: Conformationally imprinted receptors: atropisomers with “write”, “save”, and “erase” recognition properties. *Org. Lett.* **7**, 4079 (2005)
 33. Rasberry, R.D., Smith, M.D., Shimizu, K.D.: Origins of selectivity in a colorimetric charge-transfer sensor for diols. *Org. Lett.* **13**, 2889 (2008)
 34. Barooah, N., Sarma, R.J., Baruah, J.B.: Adducts of 2-hydroxyethylphthalimide with 1,3-dihydroxybenzene and 1,3,5-trihydroxybenzene. *Cryst. Growth Des.* **3**, 639 (2003)
 35. Barooah, N., Sarma, R.J., Baruah, J.B.: Solid-state hydrogen bonded assembly of *N,N'*-bis(glycyl) pyromellitic diimide with aromatic guests. *CrystEngComm* **8**, 608 (2006)
 36. Baruah, J.B., Karmakar, A., Barooah, N.: Solvent induced symmetry non-equivalence in crystal lattice of 7-carboxymethyl-1,3,6,8-tetraoxo-3,6,7,8-tetrahydro-1H-benzo[*lmn*][3,8] phenanthroline-2-yl) acetic acid. *CrystEngComm* **10**, 151 (2008)
 37. Singh, D., Baruah, J.B.: Different solvates of two isomeric dicarboxylic acids with pyridine and quinoline. *CrystEngComm* **11**, 2688 (2009)
 38. Singh, D., Bhattacharyya, P., Baruah, J.B.: Structural studies on solvates of cyclic imide tethered carboxylic acids with pyridine and quinoline. *Cryst. Growth Des.* **10**, 348 (2010)
 39. Singh, D., Baruah, J.B.: Structural study on solvates of dopamine based cyclic imide derivatives. *Cryst. Growth Des.* **11**, 768 (2011)
 40. Gawronski, J., Kaik, M., Kwit, M., Rychlewska, U.: Solvent induced folding of conformationally bistable helical imide triads. *Tetrahedron* **62**, 7866 (2006)
 41. Flamigni, L., Johnston, M.R., Giribabu, L.: Photoinduced electron transfer in bis-porphyrin di-imide complexes. *Chem. Eur. J.* **8**, 3938 (2002)
 42. Wurthner, F., Thalacker, C., Sautter, A., Schartl, W., Ibach, W., Hollricher, O.: Selforganization of perylene bisimide-melamine assemblies to fluorescent mesoscopic structures. *Chem. Eur. J.* **6**, 3871 (2000)
 43. Ji, B.M., Deng, D.S., Ma, N., Miao, S.B., Yang, X.G., Ji, L.G., Du, M.: Network formation of bis(2-benzimidazolylmethyl)amine in salts with carboxylic acids: The structures based on the interplay of strong and weak intermolecular interactions. *Cryst. Growth Des.* **10**, 3060 (2010)
 44. Goswami, S., Das, N.K., Sen, D., Fun, H.K.: Ethylene spacer-linked bisacetamidopyridine for dicarboxylic acid recognition and polymeric new wave-like antiperpendicular arrangement of a host-guest in the solid state. *Supramol. Chem.* **22**, 532 (2010)
 45. Cetina, M., Nag, A., Kristafor, V., Benci, K., Mintas, M.: The supramolecular assemblies of N-phthalimide protected (E)- and (Z)-4-amino-2-butenyl 5-substituted pyrimidine derivatives: from dimers to two-dimensional and three-dimensional networks. *Cryst. Growth Des.* **8**, 2975 (2008)
 46. Veale, E.B., Frimannsson, D.O., Lawler, M., Gunnlaugsson, T.: 4-Amino-1,8-naphthalimide based Tröger's bases as high affinity DNA targeting fluorescent supramolecular scaffolds. *Org. Lett.* **11**, 4040 (2009)
 47. Kishikawa, K., Tsubokura, S., Kohmoto, S., Yamamoto, M., Yamaguchi, K.J.: Self-assembly of *N,N'*-bis(2-tert-butylphenyl)pyromellitic diimide and phenols or indoles into a piled sandwich structure. Networks constructed by weak host-host and strong host-guest interaction in the clathrate compounds. *Org. Chem.* **64**, 7568 (1999)
 48. Kishikawa, K., Iwashima, C., Komoto, S., Yamaguchi, K., Yamamoto, M.J.: Difference in guest-inclusion abilities of *anti*- and *syn*-rotamers. *Chem. Soc. Perkin. Trans.* **1**, 2217 (2000)
 49. Aakeroy, C.B., Beatty, A.M., Helfrich, B.A.: Total synthesis in supramolecular style: Design and hydrogen-bond directed assembly of ternary cocrystals. *Angew. Chem. Int. Ed.* **40**, 3240 (2001)
 50. Aakeroy, C.B., Beatty, A.M., Helfrich, B.A.: A high-yielding supramolecular reaction. *J. Am. Chem. Soc.* **124**, 14425 (2002)
 51. Barooah, N., Baruah, J.B.: Supramolecular chemistry with phthalimide derivatives. *Mini Rev. Org. Chem.* **4**, 292 (2007)

52. Barooah, N., Sarma, R.J., Batsanov, A.S., Baruah, J.B.J.: Structural aspects of adducts of N-phthaloylglycine and its derivatives. *Mol. Struct.* **791**, 122 (2006)
53. Singh, D., Baruah, J.B.J.: Varieties in symmetry non-equivalent structural arrangements via solvation in 2-(3-methylene-1,3,7-trioxo-6-(2-carboxy-phenyl)-3,5,6,7-tetrahydro-1Hpyrrolo[3,4-f]isoindol-2-yl)benzoic acid. *Mol. Struct.* **937**, 75 (2009)
54. Sarma, B., Nath, N.K., Bhogala, B.R., Nangia, A.: Synthons competition and cooperation in molecular salts of hydroxybenzoic acids and aminopyridines. *Cryst. Growth Des.* **9**, 1546 (2009)
55. Bhogala, B.R., Nangia, A.: Ternary and quaternary co-crystals of 1,3-*cis*-5-*cis*cyclohexanetricarboxylic acid and 4,4'-bipyridines. *New J. Chem.* **32**, 800 (2008)
56. Halasz, I., Rubcic, M., Uzarevic, K., Dilovic, I., Mestrovic, E.: The cocrystal of 4-oxopimelic acid and 4,4'-bipyridine: polymorphism and solid-state transformations. *New J. Chem.* **35**, 24 (2011)
57. Koner, A.L., Schatz, J., Nau, W.M., Pischel, U.J.: Selective sensing of citrate by a supramolecular 1,8-naphthalimide/calix[4]arene assembly via complexation-modulated pKa shifts in a ternary complex. *Org. Chem.* **72**, 3889 (2007)
58. Akkus, G.U., Cebeci, C.J.: Synthesis and extraction studies of polymeric phthalimido functionalized calix[4]arene. *Incl. Phenom. Macrocycl. Chem.* **62**, 303 (2008)
59. Nangia, A., Desiraju, G.R.: Supramolecular Synthons and Pattern Recognition: Design of Organic Solids. In: Weber, E. (ed.) *Crystal Design: Structure and Function in Perspectives in Supramolecular Chemistry* vol 7. Springer-Verlag, Berlin (1998)
60. Etter, M.C., Macdonald, J.C., Bernstein, J.: Graph-set analysis of hydrogen-bond patterns in organic crystals. *Acta Crystallogr. B* **46**, 256 (1990)
61. Etter, M.C.: Encoding and decoding hydrogen-bond patterns of organic compounds. *Acc. Chem. Res.* **23**, 120 (1990)
62. Zhang, J., Huang, F., Li, N., Wang, H., Gibson, H.W., Gantzel, P., Rheingold, A.L.J.: Paraquat substituent effect on complexation with a dibenzo-24-crown-8-based cryptand. *Org. Chem.* **72**, 8935 (2007)
63. Zhu, K., Li, S., Wang, F., Huang, F.J.: Anion-controlled ion-pair recognition of paraquat by a bis(*m*-phenylene)-32-crown-10 derivative heteroditopic host. *Org. Chem.* **74**, 1322 (2009)
64. Li, S., Liu, M., Zheng, B., Zhu, K., Wang, F., Li, N., Zhao, X., Huang, F.: Taco complex templated syntheses of a cryptand/paraquat [2] rotaxane and a [2] catenane by olefin metathesis. *Org. Lett.* **11**, 3350 (2009)
65. Zaworotko, M. J.: Superstructural diversity in two dimensions: Crystal engineering of laminated solids. *Chem. Commun.* 1-9 (2001)
66. Rajput, L., Biradha, K.: Design of co-crystals via new and robust Supramolecular synthon between carboxylic-acid and secondary amide: honeycomb network with jailed aromatics. *Cryst. Growth Des.* **9**, 40 (2009)
67. Etter, M.C., Reutzel, S.M.J.: Hydrogen bond directed cocrystallization and molecular recognition properties of acyclic imides. *Am. Chem. Soc.* **113**, 2586 (1991)
68. Sheldrick, G.M.: A short history of *SHELX*. *Acta Cryst.* **A64**, 112 (2008)